Journal of Molecular Structure 1200 (2020) 127105

Contents lists available at ScienceDirect

Journal of Molecular Structure

journal homepage: http://www.elsevier.com/locate/molstruc

Effect of hydration and structure on the fragmentation of 2,2-(propane-1,3-diyl)bis(isoindoline-1,3-dione) and 2,2-(ethane-1,2-diyl) bis(isoindoline-1,3-dione) in electron impact ionization-mass spectrometry: A theoretical and experimental study

Samiyeh Yosefdad, Younes Valadbeigi*, Mohammad Bayat

Department of Chemistry, Faculty of Science, Imam Khomeini International University, Qazvin, Iran

ARTICLE INFO

Article history:
Received 4 July 2019
Received in revised form
1 September 2019
Accepted 20 September 2019
Available online 23 September 2019

Keywords:
Phthalimide derivatives
Fragmentation
Mass spectrometry
Hydration

ABSTRACT

Two bis-phthalimide derivatives, 2,2-(ethane-1,2-diyl)bis(isoindoline-1,3-dione) (**3**) and 2,2-(propane-1,3-diyl)bis(isoindoline-1,3-dione) (**4**) were synthesized and characterized by ^{1}H NMR, ^{13}C NMR and electron impact ionization-mass spectrometry (EI-MS). Effect of the alkyl length on the fragmentation of the compounds **3** and **4** was investigated and it was found that molecular ion of **3** with a CH_2—CH_2 group is almost completely decomposed, so that a small peak was observed for its molecular ion at *m/z* of 320. On the other hand, an intense peak with *m/z* of 334 was observed for the molecular ion of **4** indicating the stability of $\mathbf{4}^+$ ion. The results were interpreted using computational method at B3LYP/6-31 + G(d) level of theory. Also, comparison of the mass spectra showed that the cation $\mathbf{4}^+$ is tri-hydrated while $\mathbf{3}^+$ is not hydrated. From the optimized structures of $\mathbf{4}^+(H_2O)_{1\text{-}3}$ clusters, it was found that the extra stability of $\mathbf{4}^+(H_2O)_3$ is due to formation of hydronium ion $(H_2O)_2H_3O^+$.

1. Introduction

Phthalimide derivatives are important organic compounds having wide applications as precursors in synthesis of many classes of compounds including anthranilic acid, azo dyes, amines, peptides, and saccharin [1—3]. Also, some phthalimide derivative have pharmaceutical application and are used as drugs such as talmetoprim, thalidomide, taltrimide, and amphotalide [4—6]. Also, folpet and captan are two fungicides with phthalimide scaffold. Recently, phthalimide derivatives have been introduced as anticancer and antitumor drugs [7,8]. Hence, considerable efforts have been made to synthesize and characterize the phthalimide derivatives [9—12]. Several techniques including mass spectrometry (MS), nuclear magnetic resonance (NMR), X-ray diffraction, FT-IR and UV—Vis spectroscopy have been used for characterization of phthalimide derivatives [13—16].

Mass spectrometry is a useful technique for determination and characterization of compounds which has been used with different ion sources including electron impact (EI) ionization, electrospray ionization (ESI), photoionization, matrix-assisted laser desorption/ionization (MALDI), plasma ionization, and atmospheric pressure chemical ionization (APCI) [17—20]. EI is a hard ionization technique so that it leads to fragmentation of the parent molecule, hence, EI-MS is a useful technique for characterization of organic compounds via identification of the fragments [21,22]. The EI-MS determines the fragments of a molecule, however, combination of quantum computational methods with the experimental data provides detailed information on the structures of the studied molecules [23,24]. Also, the theoretical methods have been used for interpretation of effects of different parameters such as hydration and substitution on the strength of the bonds and their cleavage in the EI ionization source [25,26]. These studies show that hydration changes the fragmentation patterns and can protect the clusters from hard fragmentation.

In this work, two symmetric bis-phthalimide derivatives are synthesized and characterized by ^{1}H NMR, ^{13}C NMR and EI-MS. Effects of hydration and structure of the fragmentation these compounds are investigated experimentally and theoretically by density functional theory (DFT).

* Corresponding author.
E-mail addresses: valadbeigi@sci.ikiu.ac.ir, y.valadbeigi@yahoo.com (Y. Valadbeigi).

https://doi.org/10.1016/j.molstruc.2019.127105
0022-2860/

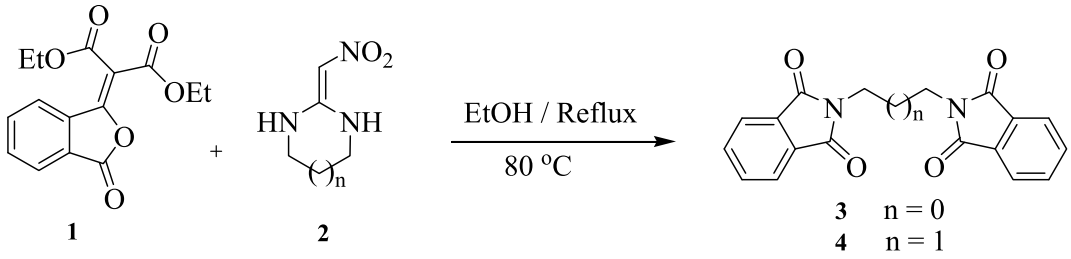

Scheme 1.

2. Experimental

2.1. General

The 1,n-diamine (GC grade: > 99%), phthalic anhydride (ACS reagent grade: > 99%), pentane-2,4-dione (GC grade: > 99%), acetic anhydride, triethylamine, ethanol (GC grade: > 99.5%), diethyl ether, hexane were obtained from Merck and Aldrich and were used without further purification. NMR spectra were recorded with a Bruker DRX-300 Avance instrument (300 MHz for ^{1}H and 75.4 MHz for ^{13}C) with DMSO as solvent. Chemical shifts are given in ppm (δ) relative to internal TMS and coupling constant (J) are reported in hertz (Hz). Melting points were measured with an electrotherma1 9100 apparatus. Mass spectra were recorded with an Agilent 5975C VL MSD with Triple-Axis Detector operating at an ionization potential of 70 eV. The samples were introduced directly to the ionization chamber. The ion source, and quadrupole temperatures were set to 230 °C, 150 °C, respectively. The probe temperature is variable depending on the melting point of samples. IR spectra were measured with a Bruker Tensor 27 spectrometer (Fig. S1 in Supplementary Materials). Elemental analyses for C, H and N were performed using a PerkinElmer 2004 series [II] CHN elemental analyzer.

2.2. General procedure for the synthesis of 3

To a solution of phthalic anhydride (1 mmol) and pentane-2,4-dione or diethyl malonate (1 mmol) in acetic anhydride (0.56 ml) at 25 °C, triethylamine (2 mmol) was added dropwise and the mixture stirred for 30 min. The reaction was quenched by the addition of aqueous hydrochloric acid (2.3 ml of 1 M solution). The resulting solid was collected by filtration, and washed with diethyl ether (1.5 ml) and then with hexane (1.5 ml) to give **1** as colorless crystals (Scheme 1). A mixture of diethyl-2-(3-oxo-2-isoindoline-1-ylidene)malonate **1** (0.30 g, 1 mmol), 2-(nitromethylene)imidazoline **2** (1 mmol) and EtOH (5 ml) in a 50 mL flask was heated at reflux for 3 h. After completion of the reaction [monitored by TLC (Thin-Layer Chromatography), ethyl acetate/n-hexane, 1:1], the reaction mixture was cooled to room temperature and the formed solid filtered. The solid was washed with ethanol or recrystallized from ethanol to give pure product **3** in high yield.

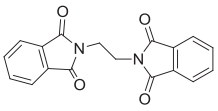

(3) : 1.2.2. *2,2-(ethane-1,2-diyl)bis(isoindoline-1,3-dione)*

White powder; yield: 0.43 g (82%); m.p. 245–247 °C. ^{1}H NMR (300 MHz, DMSO): 4.10 (2H, d, CH_2), 7.71 (2H, m, ArH), 7.80 (2H, m, ArH). ^{13}C NMR (75.4 MHz, DMSO): 38.8, 123.3, 131.9, 134.0, 168.3. IR (KBr) (υ_{max}/cm^{-1}): 3274, 2062, 1631, 1200, 650. Anal. Calcd for $C_{18}H_{12}N_2O_4$ (320.30): C, 67.50; H, 3.78; N, 8.75. Found: C, 67.8; H, 3.5, N, 8.6.

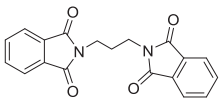

(4) : 1.2.1. *2,2-(propane-1,3-diyl)bis(isoindoline-1,3-dione)*

White powder; yield: 0.36 g (70%); m.p. 204–206 °C. ^{1}H NMR (300 MHz, DMSO): 2.10 (2H, p, $^{3}J_{HH} = 7.4$ Hz, CH_2), 3.78 (2H, t, $^{3}J_{HH} = 7.4$ Hz, CH_2), 7.71 (2H, m, ArH), 7.80 (2H, m, ArH). ^{13}C NMR (75.4 MHz, DMSO): 27.6, 35.7, 123.3, 132.1, 134.0, 168.2. IR (KBr) (υ_{max}/cm^{-1}): 2946, 1710, 1390, 1173, 1019, 720. Anal. Calcd for $C_{19}H_{14}N_2O_4$ (334.33): C, 68.26; H, 4.22; N, 8.38. Found: C, 68.6; H, 4.4, N, 8.2.

2.3. Computational details

Structures of the neutral and cationic molecules as well as the hydrated species were fully optimized by density functional theory employing B3LYP functional. The basis set 6-31 + G(d) including diffuse and polarization functions were used for the calculations. Also, the larger basis set 6–31++G(d,p) was used for computing thermodynamic data of the hydration reactions. The frequency calculations were performed at the smae level to calculate the thermodynamic quantities such as enthalpy (ΔH) and Gibbs free energy (ΔG) values of hydration. Both the vertical (VIE) and adiabatic ionization energies (AIE) for the compounds **3** and **4** were calculated at the same level of theory. In the case of VIE, the structure of the neutral compound (M) was optimized and the same geometry was used for its corresponding cation (M^+). For the AIE, the structures of both M and M^+ were optimized. The calculations in solvent (chloroform) were performed by Tomasi's Polarized Continuum Model (PCM) [27] at the same level of theory. All calculations were carried out using Gaussian 09 software [28].

3. Result and discussion

3.1. Effect of structure on the fragmentation of 3 and 4

Fig. 1 shows the structures of the compounds **3** and **4**, optimized in gas phases. Two isomers, **a** and **b**, for each compounds were considered. The isomers **3b** and **4b** are more stable in gas phase, while the stability of the isomers **3a** and **4a** increases in $CHCl_3$

solvent. However, the energy difference of the isomers in both gas phase and $CHCl_3$ solvent is not considerable and their stabilities are comparable.

Figs. S2–S5 (Supplementary Materials) show the ^1H NMR and ^{13}C NMR spectra of the compounds **3** and **4**. For comparison, the computationally obtained NMR spectra of these compounds have been shown in Figs. S2–S5. The experimental and theoretical NMR spectra are in good agreement with each other.

Fig. 2 shows the EI-MS spectra of the compounds **3** and **4**. The fragmentation patterns for the compounds **3** and **4** are almost the same, however, for the compounds **3**, the molecular ion (parent ion) peak with *m/z* of 320 is very small. In contrast, the MS spectra of **4** shows a sharp peak for the parent ion, $M^{+\cdot}$ with *m/z* of 334. The calculated ionization energies for these compounds (Table S1) are approximately equal. It seems, the number of CH_2 groups between the phthalimide moieties is responsible for different fragmentation of the compounds **3** and **4**.

Fig. 3 compares the C–C and N–C bond lengths in the neutral **3** and **4** and their cationic forms, $\mathbf{3}^+$ and $\mathbf{4}^+$. Ionization of **4** does not lead in considerable change in the C–C and N–C bond lengths so that the changes in the C–C and N–C upon ionization are 0.024 and 0.023 Å, respectively. On the other hands, ionization of **3** leads to larger change in the C–C and N–C bond lengths, 0.091 and 0.047 Å, respectively. The larger bond change in **3** after ionization increases the possibility of fragmentation, hence, its parent ion peak is not observed. In the $\mathbf{3}^+$, with two CH_2 groups, the N atom donates its lone pair to the carbons of the CH_2 groups to relieve and accommodate some of the positive charge of C atoms. Hence, the N–C bond become shorter and obtains a nature between single, N–C, and double bonds, N=C. Also, the H–C–H angle change from 109.5° in neutral **3** to 113.1° in $\mathbf{3}^+$. This weakens the H_2C–CH_2 bond and induces its fragmentation so that an intense peak is observed in *m/z* of 160 for symmetric cleavage of $\mathbf{3}^+$.

In the case of $\mathbf{4}^+$, the positive charge is distributed on the larger number of atoms, especially on the middle CH_2 group (Fig. S6 in Supplementary Materials) and the role of N atoms for donating their lone pair and accommodate the positive charge fades. We investigated the effect of alkyl chain length on the C–C and N–C bond lengths in different cations of phthalimide derivatives (Fig. S7). The optimized structures of these cations show that as the length of the alkyl chain increases the C–C bond length shortens and the N–C bond length is elongated. From these theoretical results it is concluded that as the alkyl chain lengthens, the C–C bond strengthen and the N–C bond is weakened. The H–C–H angles of the middle and lateral CH_2 groups of $\mathbf{4}^+$ are 109.5 and 110.7°, respectively, indicating the least changes in the nature of the bonds. Hence, the probability of $\mathbf{4}^+$ fragmentation is smaller than that of $\mathbf{3}^+$ and an intense peak is observed for the intact ion of $\mathbf{4}^+$ in *m/z* of 334. Also, the peak appeared at *m/z* of 335 may be attributed to the protonated form of **4**, $(\mathbf{4}+H)^+$.

Figs. 4 and 5 show the suggested paths for fragmentation of **3** and **4**, respectively. The possible structural isomers of the fragments have been considered and their relative stabilities have been compared. The peaks with *m/z* of 146 and 147 are due to phthalimide fragments, $C_8H_4NO_2$ and $C_8H_5NO_2$, (fragments **6** and **15**) [29,30] which can be produced directly from the $\mathbf{4}^+$ and $\mathbf{3}^+$, respectively.

Beside the common fragments of **3** and **4**, generally, fragmentation of **4** results in fragments having an extra hydrogen atoms: fragments with *m/z* of 147, 161, and 174 in the **4** spectrum versus those with *m/z* of 146, 160, and 173 in the **3** spectrum. The difference is due to tautomersim or intramolecular proton transfer in the parent cations $\mathbf{3}^+$ and $\mathbf{4}^+$. Figs. 4 and 5 show that beside keto forms, $\mathbf{3}^+$ and $\mathbf{4}^+$ have also enolic tautomers, $\mathbf{3}^+\mathbf{b}$, $\mathbf{4}^+\mathbf{b}$, and $\mathbf{4}^+\mathbf{c}$. In the enolic tautomers $\mathbf{3}^+\mathbf{b}$ and $\mathbf{4}^+\mathbf{c}$, the N–CH bond is stronger than N–CH_2 bonds in the keto tautomers, $\mathbf{3}^+\mathbf{a}$ and $\mathbf{4}^+\mathbf{a}$ (the N–C bond lengths in the keto and enol isomers have been compared Fig. S8). Hence, the N–CH_2 bond is broken more easily than N–CH bond in all tautomers. The N–CH_2 cleavage in compound **3** leads in fragments **5**, **6**, and **7** the peaks with *m/z* of 173, 146, and 160 (Fig. 4) while N–CH_2 cleavage in compound **4** produces fragments **12**, **15**, and **14** with *m/z* of 174, 147, and 161, respectively. For example, the

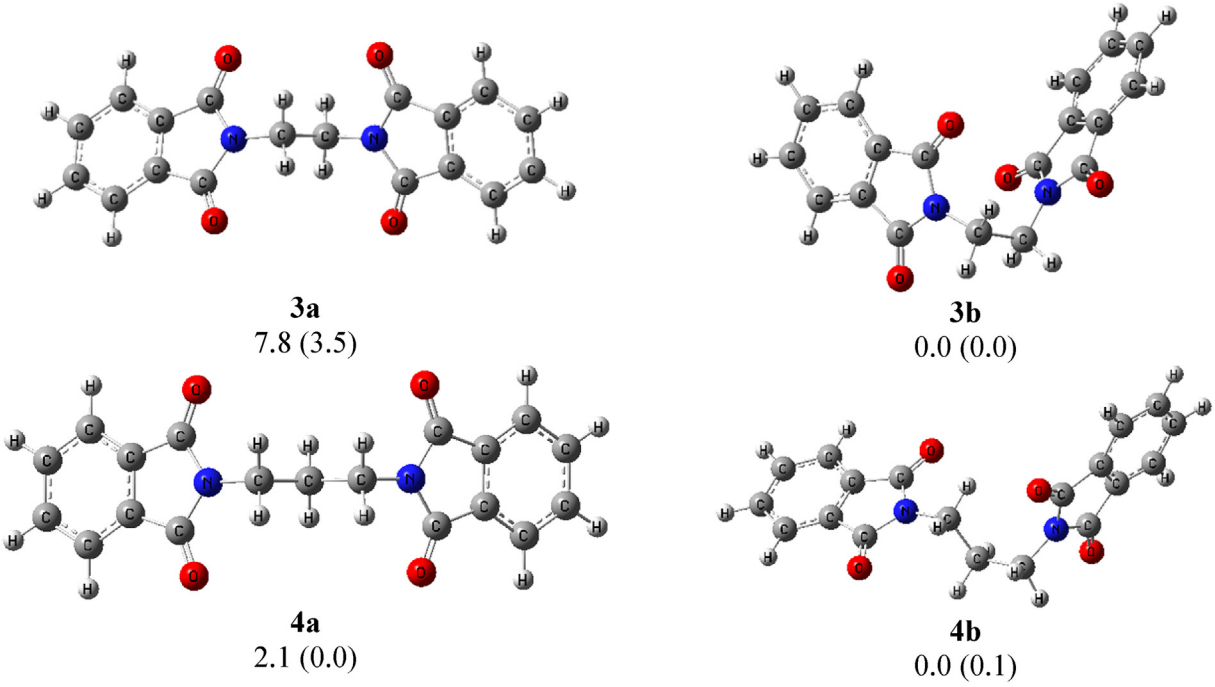

Fig. 1. Optimized structures of two isomers of compounds **3** and **4** and comparison of the relative energies of the isomers in gas phase and in $CHCl_3$ solvent. The data in parenthesis are relative energies in $CHCl_3$ solvent. The energies are in kJ mol^{-1}.

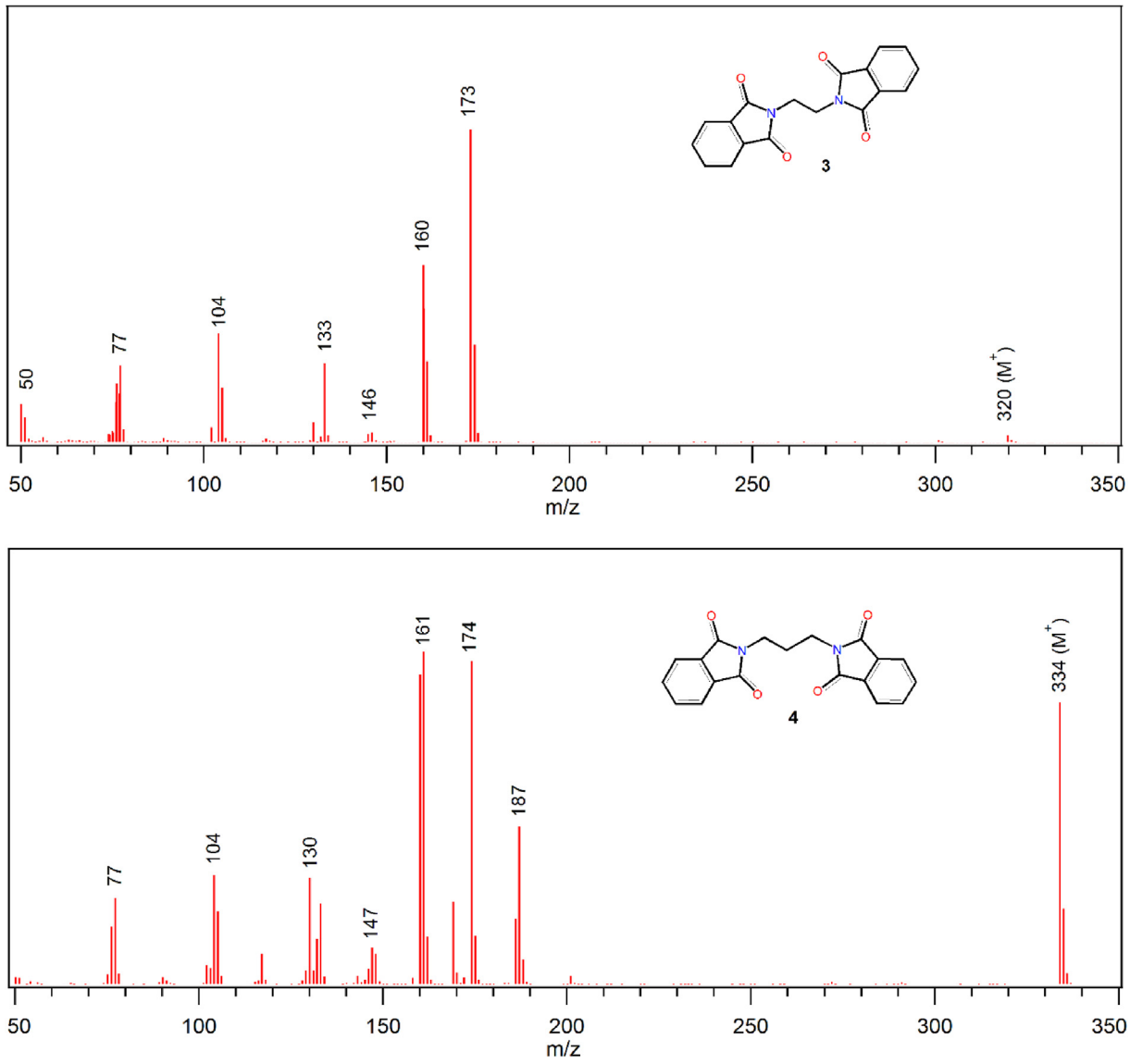

Fig. 2. The MS spectra for compounds **3** and **4** recorded with EI-MS.

calculated ΔH values for formation of **5a** (173) and **12a** (174) form $\mathbf{3}^{+}\mathbf{b}$ are

$$\mathbf{3}^{+}\mathbf{b} \rightarrow C_8O_2NH_5 + \mathbf{5a}\ (m/z = 173),\ \Delta H = 79.0\ \text{kJ mol}^{-1} \quad (1)$$

$$\mathbf{3}^{+}\mathbf{b} \rightarrow C_8O_2NH_4 + \mathbf{12a}\ (m/z = 174),\ \Delta H = 250.6\ \text{kJ mol}^{-1} \quad (2)$$

Comparison of the ΔH values reveals that formation of **5a** from $\mathbf{3}^{+}\mathbf{b}$ is thermodynamically more favored.

In the case of cation $\mathbf{4}^{+}$, the enolic tautomer $\mathbf{4}^{+}\mathbf{b}$ has no strong N–CH bond because the oxygen atom has captured the H atom of the middle CH_2. Hence, the N–C cleavage can occur simply leading in fragments **11**, **12**, **13**, **14**, and **15** with *m/z* of 188, 174, 187, 161, and 147, respectively (Fig. 5). The fragment **12** can be also formed from the fragmentation of the tautomer $\mathbf{4}^{+}\mathbf{c}$:

$$\mathbf{4}^{+}\mathbf{c} \rightarrow \mathbf{12a}\ (m/z = 174) + C_9O_2NH_6,\ \Delta H = 142.0\ \text{kJ mol}^{-1} \quad (3)$$

Comparison of the ΔH values of reactions (2) and (3) shows that, formation of the fragment **12** (*m/z* = 174) from $\mathbf{4}^{+}\mathbf{c}$ is thermodynamically more feasible.

Both the MS spectra of **3** and **4** show a peak at *m/z* of 133. This peak has been observed by other authors working on the fragmentation of phthalimide derivatives [30] and attributed to methoxybenzonitrile, fragment **17e**. However, we consider six possible isomers for fragment **17** (Fig. 5) and the calculations show that the structure **17d** is the most stable isomer. Another possible fragment with *m/z* of 133 is fragment **9** with two possible isomers (Fig. 4). The fragments **9** and **17** can be produced from both the larger fragments **7** (*m/z* = 160) and fragment **14** (*m/z* = 161) by loss of HCN and CO, respectively, hence, a common peak with *m/z* of 133 is observed in both the spectra of **3** and **4**. Although the peak with *m/z* of 130 is observed in both spectra, its intensity is considerably more in the spectrum of **4**. This peak may be assigned to fragments **8** (C_8H_4NO) and **16** (C_9H_8N).

The peak with *m/z* of 187 is observed only in the spectrum of **4** because it is due to a phthalimide moiety bearing a C_3H_5 group (fragment **13**). Four possible structural isomers were considered for fragment **13**, however, the isomer with the –CH=CH–CH_3 group, **13b**, was more stable (Fig. 5). The peak with *m/z* of 104 is present in

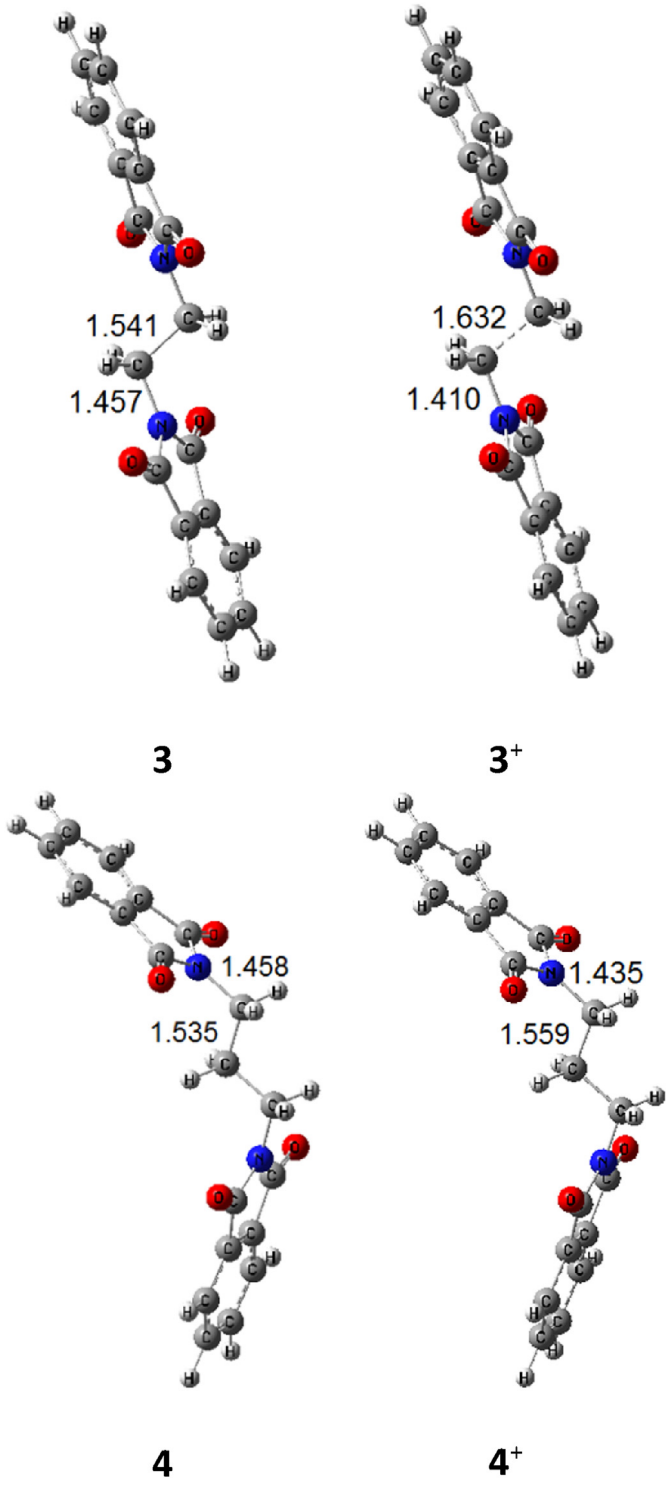

Fig. 3. Change in the C–C and N–C bond lengths in **3** and **4** compounds upon ionization. The bond lengths are in Å.

both spectra of Fig. 2 and has been reported previously for the phthalimide derivatives [30]. This peak may due to fragment **10**, C_7H_4O, with two possible isomers (Fig. 4) or fragment **19**, C_7H_6N (Fig. 5), [31]. The optimized structures of all fragments of the compounds **3** and **4** have been provided in Fig. S9 (Supplementary Materials).

3.2. Effect of hydration on the fragmentation of 3 and 4

The ethanol used as solvent for synthesis of the compounds **3** and **4** contained some water impurity and also during the synthesis some water was produced because of condensation. Fig. 6 compares the MS spectra of **4** before and after drying by oven. Before drying, the sample contains some water content and hydrated ions can be produced.

Fig. 6 shows a peak with *m/z* of 388 for wet **4** which is attributed to $\mathbf{4}^+(H_2O)_3$. We did not observe the mono- and di-hydrated cations, $\mathbf{4}^+(H_2O)$ and $\mathbf{4}^+(H_2O)_2$, that was strange at first. Also, the same experiment was repeated for **3**, and interestingly, the MS spectra of the dry and wet **3** were the same so that no hydrated cation was observed indicating that the $\mathbf{3}^+$ cation is fragmented before hydration or $\mathbf{3}^+$ is not hydrated.

To explore these results in details, hydrations of cations $\mathbf{3}^+$ and $\mathbf{4}^+$ with up to 3 water molecules were studied, theoretically. Fig. 7 shows the hydrated forms of the cations $\mathbf{3}^+$ and $\mathbf{4}^+$, $\mathbf{3}^+(H_2O)_{1\text{-}3}$ and $\mathbf{4}^+(H_2O)_{1\text{-}3}$, respectively, optimized by B3LYP/6-31 + G(d) method. The cations $\mathbf{3}^+$ and $\mathbf{4}^+$ are hydrated via hydrogen bonding interactions between the hydrogen atoms of H_2O and carbonyl oxygen of $\mathbf{3}^+$ and $\mathbf{4}^+$ and hydrogen atoms of CH_2 groups and oxygen atom of H_2O. However, the tri-hydration of $\mathbf{4}^+$ is different because the water molecules capture a hydrogen atom from a lateral CH_2 group and form a hydronium ion $(H_2O)H_3O^+$. If fact, the tri-hydrated form of $\mathbf{4}^+$ is as $[(\mathbf{4}\text{-H})(H_2O)_2H_3O]^+$. The calculated values of ΔH and ΔG for hydration of the $\mathbf{3}^+$ and $\mathbf{4}^+$ cations are summarized in Table 1. Although the ΔH values are negative, the ΔG values show that hydration of $\mathbf{3}^+$ is not thermodynamically favored and $\mathbf{3}^+$ is not hydrated. Also, comparison of the ΔG values for hydration of $\mathbf{4}^+$ shows that mono- and di-hydration of $\mathbf{4}^+$ is not thermodynamically possible while $\mathbf{4}^+(H_2O)_3$ is easily produced. The more stability of $\mathbf{4}^+(H_2O)_3$ cluster can be attributed to stronger hydrogen bonding interactions in the hydronium ion, $(H_2O)_2H_3O^+$ what is absent in $\mathbf{4}^+(H_2O)_1$ and $\mathbf{4}^+(H_2O)_2$. The calculated thermodynamic results are in excellent agreement with the MS spectrum of wet **4** so that we observed only one peak with *m/z* of 388 for $\mathbf{4}^+(H_2O)_3$ and the peaks of $\mathbf{4}^+(H_2O)_1$ and $\mathbf{4}^+(H_2O)_2$ with *m/z* of 352 and 370, respectively, did not appear. Also, the data in Table 1 show that $\mathbf{3}^+$ is not hydrated and we observed the same spectrum patterns for the wet and dry **3** (not shown).

Another structural feature of the hydrated cations is change in the $H_2C\text{—}CH_2$ bond length of $\mathbf{3}^+$ upon hydration. The C—C bond length is elongated due to ionization from 1.54 in **3** to 1.63 Å in $\mathbf{3}^+$ (Fig. 3) and hydration elongates more the C—C bond to 1.65 Å (Fig. 7). The effect of hydration on the C—C bond length in the $\mathbf{4}^+$ cation is negligible. Hence, hydration does not increase the fragmentation of $\mathbf{4}^+$. However, new peaks between the peaks 187 and 334 appear for the wet **4** indicating that hydration influences the mechanism of fragmentation. Fig. 8 shows the proposed paths for formation of fragments 18 and 19 with *m/z* of 315 and 287, respectively, from $\mathbf{4}^+(H_2O)_3$. According to this suggested mechanism, $\mathbf{4}^+$ is tri-hydrated, $\mathbf{4}^+(H_2O)_3$, then the water molecules capture an H atom from $\mathbf{4}^+$ to form $[(\mathbf{4}\text{-H})(H_2O)H_3O]^+$ (Fig. 7) with *m/z* of 388. During the dehydration, the complex $[(\mathbf{4}\text{-H})(H_2O)_2H_3O]^+$ loses four water molecules instead of three water molecules to produce fragment 18 with *m/z* of 315. In other words, the $\mathbf{4}^+$ obtains three H_2O and loses four H_2O molecules so that the primary three water molecules can catalyze loss of an extra water molecule. Another straightforward path is dehydration of $(\mathbf{4}\text{-H})^+$ and formation of $(\mathbf{4}\text{-}H_3O)^+$, **20**, without assistance of the hydrating water molecules. However, in both paths, presence of the hydrating water molecules for formation of **20** with *m/z* of 315 is necessary. The fragment **21** with *m/z* of 287 is produced from fragment **20** by loss of a CO group. Other fragments with *m/z* of 268 (**22**) and 241 (**23**)

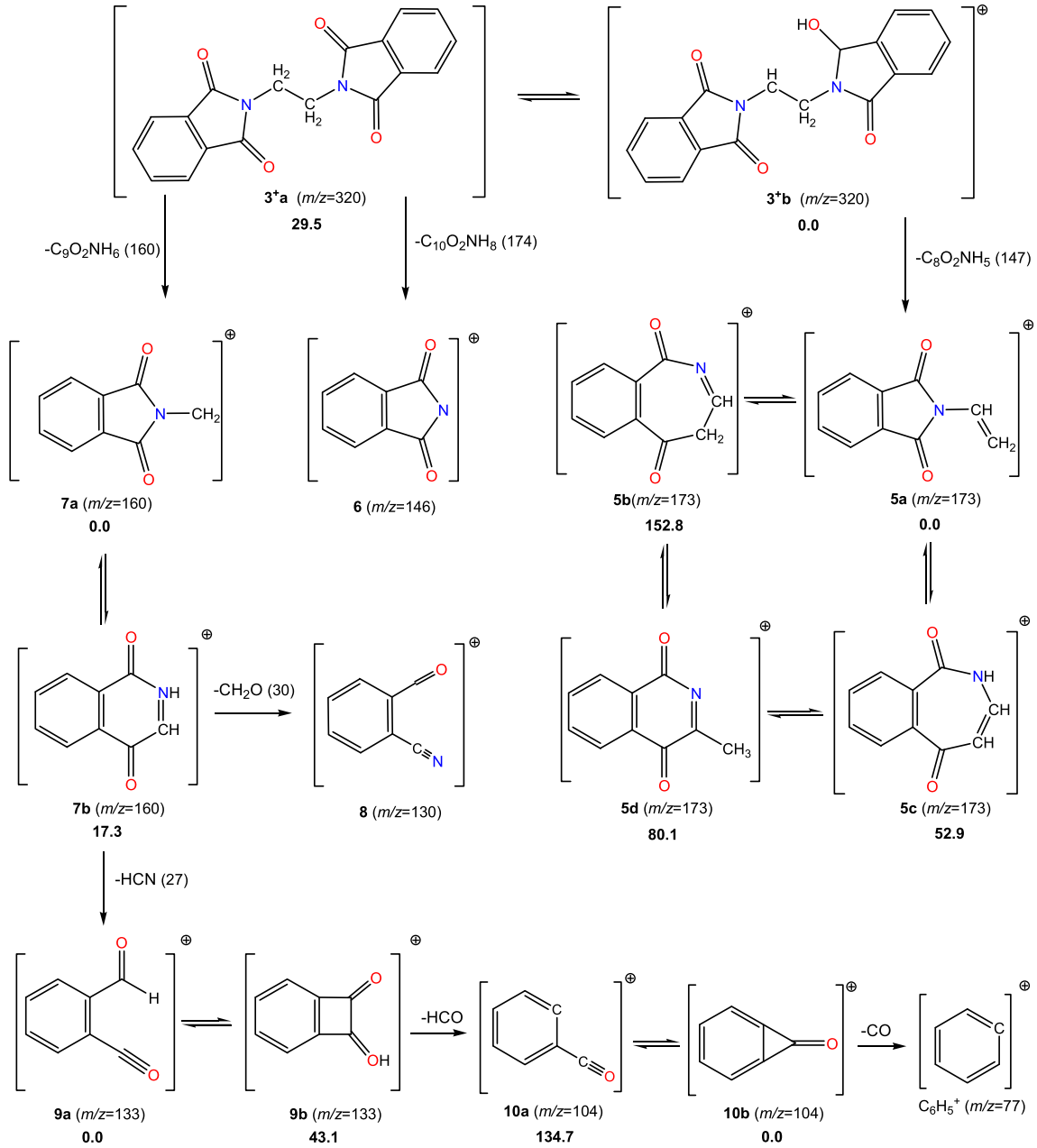

Fig. 4. The proposed paths for fragmentation of $\mathbf{3}^+$ in EI-MS. The bold numbers are relative energies in kJ mol^{-1}.

are formed from **21** by consecutive loss of H_2O and CO. Also, the observed peak at *m/z* of 342 may be due to $[M\text{-}CO+2H_2O]^+$. The optimized structures of the fragments **20**–**23** have been shown in Fig. S10 (Supplementary Materials).

4. Conclusion

The phthalimide derivatives **3** and **4** were synthesized and their structures were characterized by ^1H NMR, ^{13}C NMR and EI-MS. Ionization and fragmentation of **3** and **4** in electron impact ionization source were studied both experimentally by mass spectrometry and theoretically using DFT calculations. It was found that fragmentation of the compounds **3** and **4** and consequently their MS spectra patterns depend on both structure and hydration while hydration itself depends on the structure. The molecular ion of **3** with an N–$(CH_2)_2$–N group was almost completely decomposed so that we observed only a small peak for its molecular ion, M^+, with *m/z* of 320. In contrast, for the **4** with a longer alkyl chain, N–$(CH_2)_3$–N, an intense peak was observed for the molecular ion peak at *m/z* of 334. These results were interpreted theoretically using charge distribution analysis and change in the bond strengths. Effect of hydration on the ionization and fragmentation of $\mathbf{3}^+$ and $\mathbf{4}^+$ was studied and it was found that $\mathbf{3}^+$ is not hydrated and consequently hydration does not influence its fragmentation mechanism. The MS spectra showed that $\mathbf{4}^+$ is tri-hydrated, $\mathbf{4}^+(H_2O)_3$, and theoretical results confirmed that only tri-hydration of $\mathbf{4}^+$ is thermodynamically possible while $\mathbf{4}^+(H_2O)_1$ and $\mathbf{4}^+(H_2O)_2$ were not stable. Also, hydration of $\mathbf{4}^+$ leaded to appearance of some new peaks, hence, it was concluded that hydration influences the fragmentation mechanism of $\mathbf{4}^+$. The optimized structure of tri-hydrated form of $\mathbf{4}^+$ revealed that the water molecules capture one of the hydrogen atoms of CH_2 group so that

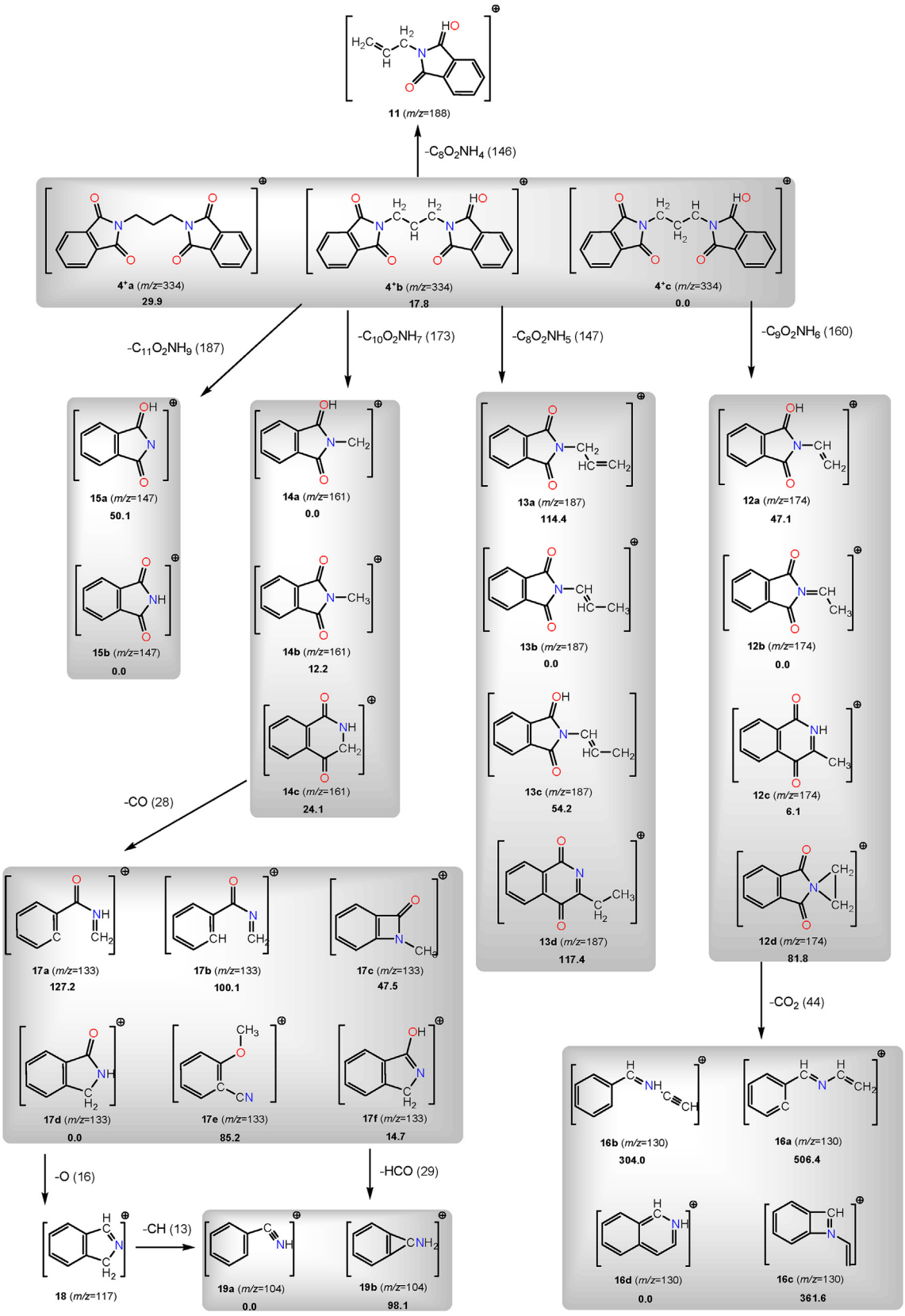

Fig. 5. The proposed paths for fragmentation of $\mathbf{4}^{+}$ in EI-MS. The bold numbers are relative energies in kJ mol^{-1}.

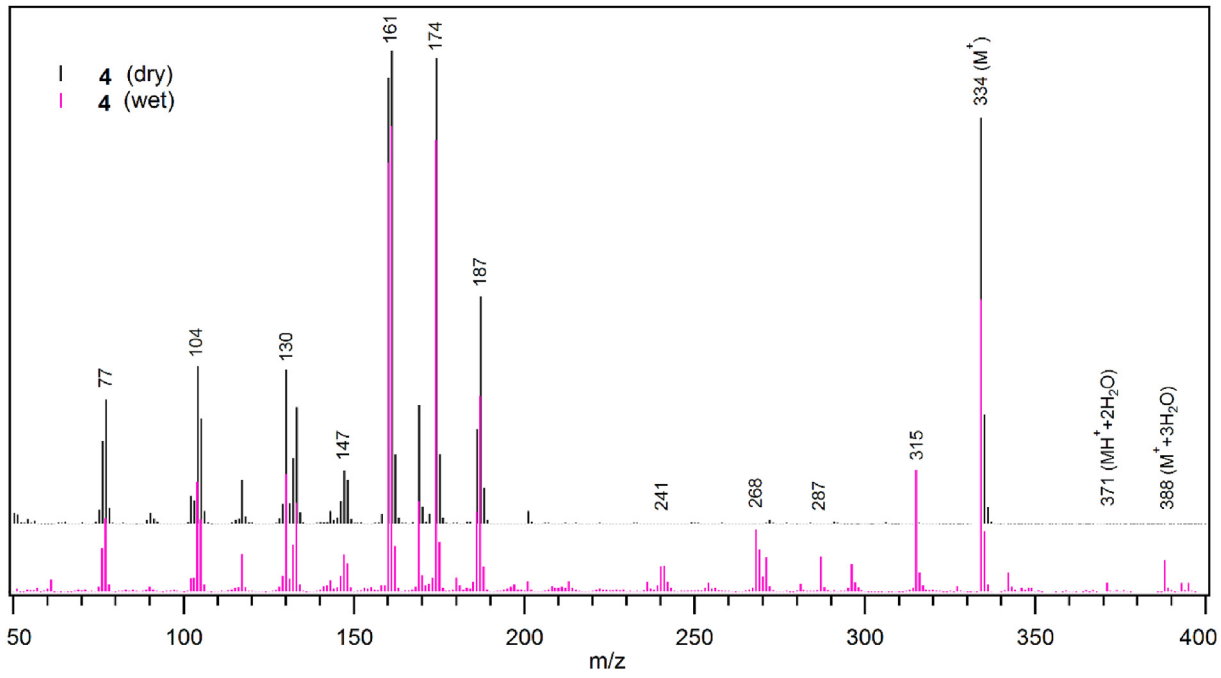

Fig. 6. Effect of hydration of the spectrum pattern: Comparison of the MS spectra of dry and wet **4**.

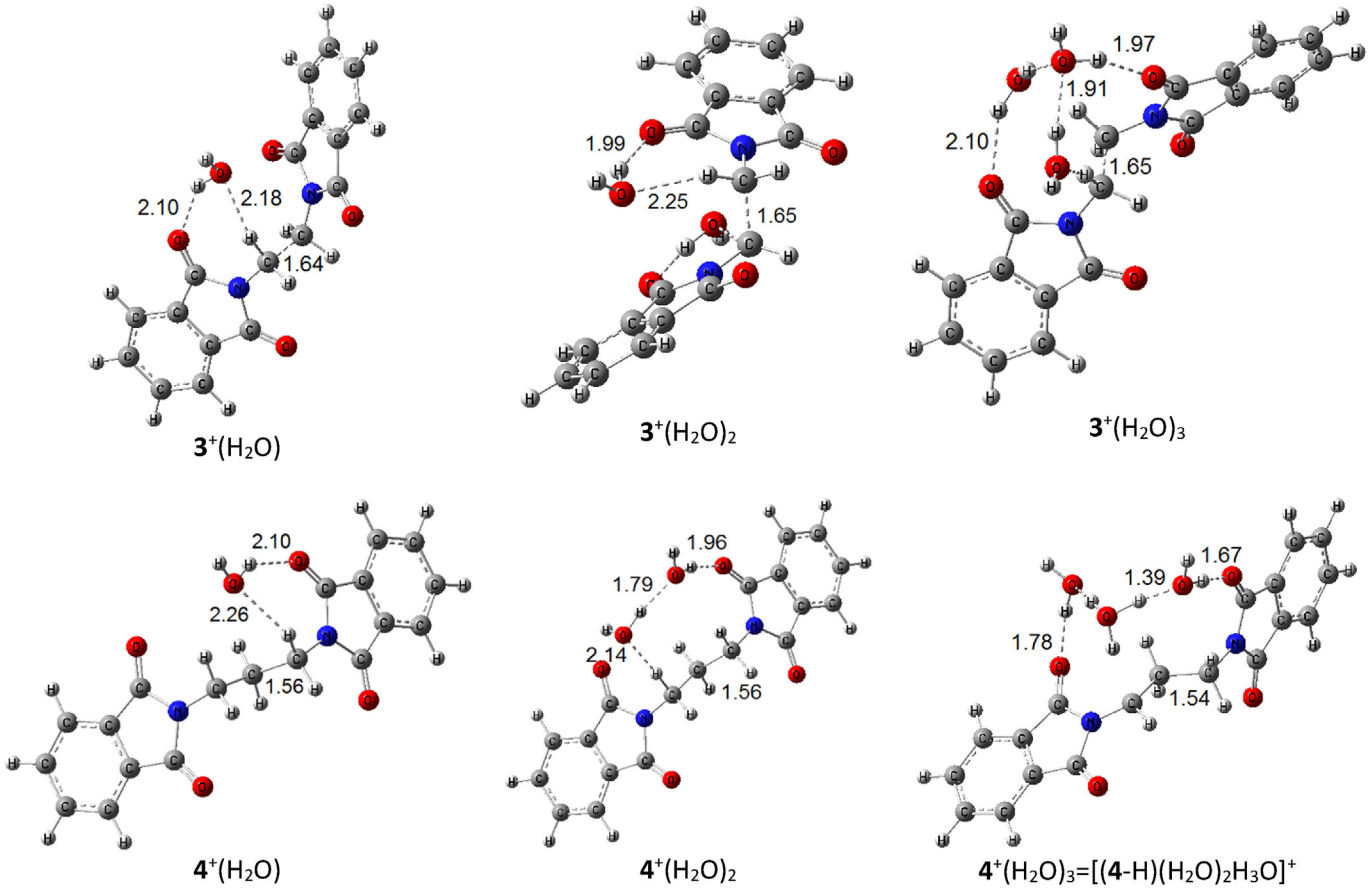

Fig. 7. The optimized structures of the hydrated forms of the $\mathbf{3}^{+}$ and $\mathbf{4}^{+}$ cations. The bond lengths are in Å.

the final complex is as $[(\mathbf{4}\text{-H})(H_2O)_2H_3O]^{+}$. The appearance of the new peaks in MS spectrum of wet **4** was attributed to hydrogen abstraction from $\mathbf{4}^{+}$ by the water molecules.

Table 1
The ΔH and ΔG values for hydration of the $\mathbf{3}^+$ and $\mathbf{4}^+$ cations in gas phase at 298 K, calculated at B3LYP/6-31 + G(d) level. The data in parenthesis have been calculated using 6−31++G(d,p) basis set.

Hydration	ΔH (kJ mol^{-1})	ΔG (kJ mol^{-1})
$\mathbf{3}^+ + H_2O \rightarrow \mathbf{3}^+(H_2O)$	−32.9 (−31.3)	6.4 (8.5)
$\mathbf{3}^+(H_2O) + H_2O \rightarrow \mathbf{3}^+(H_2O)_2$	−36.2 (−30.7)	5.2 (5.2)
$\mathbf{3}^+(H_2O)_2 + H_2O \rightarrow \mathbf{3}^+(H_2O)_3$	−30.1 (−31.8)	7.7 (8.7)
$\mathbf{4}^+ + H_2O \rightarrow \mathbf{4}^+(H_2O)$	−29.3 (−28.6)	8.5 (9.0)
$\mathbf{4}^+(H_2O) + H_2O \rightarrow \mathbf{4}(H_2O)_2$	−37.6 (−35.9)	−0.9 (−0.2)
$\mathbf{4}^+(H_2O)_2 + H_2O \rightarrow \mathbf{4}^+(H_2O)_3$	−106.0 (−119.1)	−49.5 (−62.6)

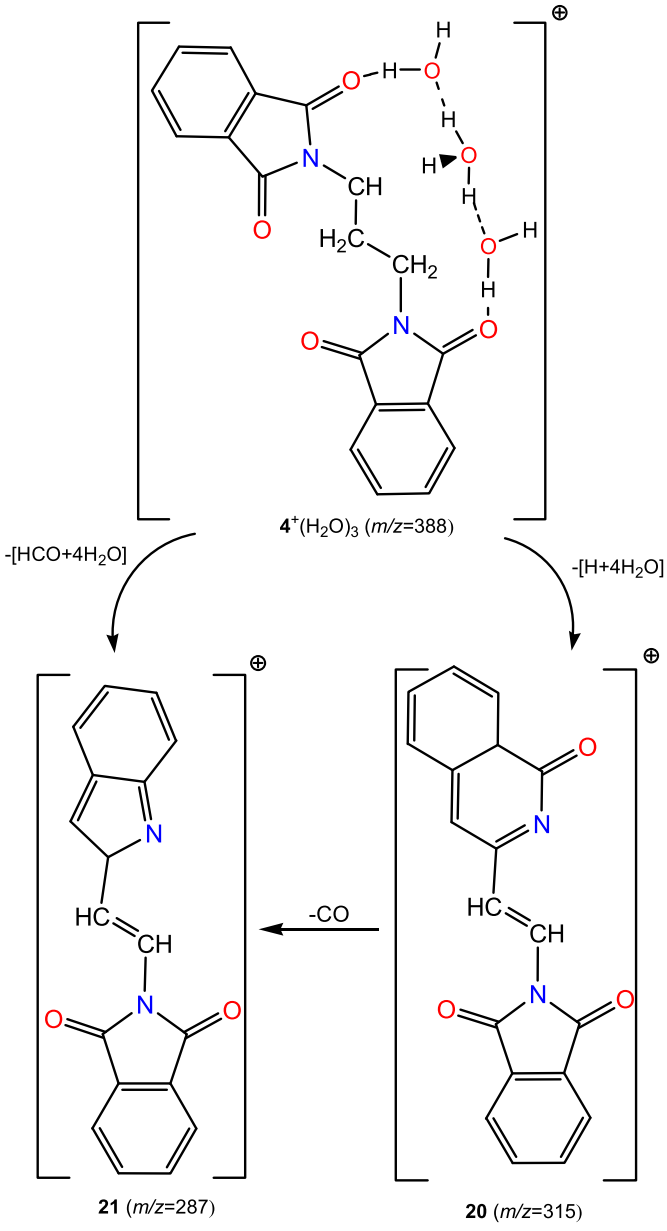

Fig. 8. The proposed paths for formation of fragments **20** and **21** with *m/z* of 315 and 287, respectively, from $\mathbf{3a}^+(H_2O)_3$.

Acknowledgments

Y.V. thanks HPC Computing Facility of IKIU, Iran, for computational resources.

Appendix A. Supplementary data

Supplementary data to this article can be found online at https://doi.org/10.1016/j.molstruc.2019.127105.

References

[1] J.S. Koh, J.P. Kim, Synthesis of phthalimide-based alkali-dischargeable azo disperse dyes and analysis of their alkali-hydrolysis mechanism, Dyes Pigments 37 (1998) 265−272.
[2] G.H. Imanzadeh, A. Khalafi-Nezhad, A. Zare, A. Hasaninejad, A.R. Moosavi Zare, A. Parhami, Michael addition of phthalimide and saccharin to α,β-unsaturated esters under solvent-free condition, J. Iran. Chem. Soc. 4 (2007) 229−237.
[3] X. Zhao, Study on hydrolysis performance of phthalimide disperse dyes, Dyes Pigments 163 (2019) 600−606.
[4] L.M. Lima, P. Castro, A.L. Machado, C.A.M. Fraga, C. Lugnier, V. Lucia, G. de Moraes, E.J. Barreiro, Synthesis and anti-inflammatory activity of phthalimide derivatives, designed as new thalidomide analogues, Bioorg. Med. Chem. 10 (2002) 3067−3073.
[5] J.V. Ragavendran, D. Sriram, S.K. Patel, I.V. Reddy, N. Bharathwajan, J. Stables, P. Yogeeswari, Design and synthesis of anticonvulsants from a combined phthalimide-GABA-anilide and hydrazine pharmacophere, Eur. J. Med. Chem. 42 (2007) 146−151.
[6] R. Antunes, H. Batista, R.M. Srivastava, G. Thomas, C.C. Araujo, R.L. Longo, H. Magalhaes, M.B.C. Leao, A.C. Pavao, Synthesis, characterization and interaction mechanism of new oxadiazolo-phthalimides as peripheral analgesics. IV, J. Mol. Struct. 660 (2003) 1−13.
[7] C. Pessoa, et al., Discovery of phthalimides as immunomodulatory and anti-tumor drug prototypes, ChemMedChem 5 (2010) 523−528.
[8] S.H. Chan, et al., The preparation and in vitro antiproliferative activity of phthalimide based ketones on MDAMB-231 and SKHep-1 human carcinoma cell lines, Eur. J. Med. Chem. 44 (2009) 2736−2740.
[9] S.M. Capitosti, T.P. Hansen, M.L. Brown, Facile synthesis of an azido-labeled thalidomide analogue, Org. Lett. 5 (2003) 2865−2867.
[10] J. Lohbeck, A.K. Miller, Practical synthesis of phthalimide-based cereblon ligand to enable PROTAC development, Bioorg. Med. Chem. Lett 26 (2016) 5260−5262.
[11] C. Shinji, T. Nakamura, S. Maeda, M. Yoshida, Y. Hashimoto, H. Miyachi, Design and synthesis of phthalimide-type histone deacetylase inhibitors, Bioorg. Med. Chem. Lett 15 (2005) 4427−4431.
[12] D.J. Rao, D. Rajaniverma, P.V. Prasannakumar, V. Seetaramaiah, Y. Ramakrishna, Phthalimide from 2-acetyl-benzoic acid: spectroscopy and quantum chemical studies, J. Mol. Struct. 1186 (2019) 482−489.
[13] S. Torrico-Vallejos, M.F. Erben, O.E. Piro, E.E. Castellano, C.O.D. Vedova, Vibrational properties, crystal X-ray diffraction structure and quantum chemical calculations on a divalent sulfur substituted phthalimide: 1H-Isoindole-1,3(2H)-dione, 2-[(methoxycarbonyl)thio], J. Mol. Struct. 975 (2010) 227−233.
[14] R. Arif, P.S. Nayab, P. Rashisuddin, Synthesis, Characterization, DNA binding, antibacterial, and antioxidant activity of new bis-phthalimides, Russ. J. Gen. Chem. 86 (2016) 1374−1380.
[15] Y. Lingappa, S.S. Rao, R.V.S.S.N. Ravikumar, P.S. Rao, Synthesis, characterization and biological activity of phthalimide derivatives of Cu(II) complex, Radiat. Eff. Defects Solids 162 (2007) 11−16.
[16] A. Weisz, D. Andrzejwski, A. Mandelbaum, Fragmentation of isomeric N-Quinolinyl-phthalimides on electron impact ionization, J. Mass Spectrom. 31 (1996) 676−680.
[17] N. Mirsaleh-Kohan, W.D. Roberson, Electron ionization time-of-flight mass spectrometry: historical review and current applications, Mass Spectrom. Rev. 27 (2008) 237−285.
[18] C. Bhardwaj, L. Hnley, Ion sources for mass spectrometric identification and imaging of molecular species, Nat. Prod. Rep. 31 (2014) 756−767.
[19] C.N. McEwen, B.S. Larsen, Fifty years of desorption ionization of nonvolatile compounds, Int. J. Mass Spectrom. 377 (2015) 515−531.
[20] Y. Valadbeigi, V. Ilbeigi, B. Michalczuk, M. Sabo, S. Matejcik, Study of atmospheric pressure chemical ionization mechanism in corona discharge ion source with and without NH3 dopant by ion mobility spectrometry combined with mass spectrometry: a theoretical and experimental study, J. Phys. Chem. A 123 (2019) 313−322.
[21] F.J. Arrebola, J.L. Martinez Vidal, M. Mateu-Sanchez, F.J. Castellon, Determination of 81 multiclass pesticides in fresh foodstuffs by a single injection analysis using gas chromatography-chemical ionization and electron ionization tandem mass spectrometry, Anal. Chim. Acta 484 (2003) 167−180.
[22] A.C. Aiken, P.F. DeCarlo, J.L. Jimenez, Elemental analysis of organic species with electron ionization high-resolution mass spectrometry, Anal. Chem. 79 (2007) 8350−8358.
[23] S. Grimme, Towards first principles calculation of electron impact mass spectrometry, Angew. Chem. Int. Ed. 52 (2013) 6306−6312.
[24] P. Wright, A. Alex, T. Nyaruwata, T. Parsons, F. Pullen, Using density functional theory to rationalize the mass spectral fragmentation of maraviroc and its metabolites, Rapid Commun. Mass Spectrom. 24 (2010) 1025−1031.
[25] M. Neustetter, M. Mahmoodi-Darian, S. Denifl, Study of electron ionization and fragmentation of non-hydrated and hydrated tetrahydrofuran clusters,

J. Am. Soc. Mass Spectrom. 28 (2017) 866–872.
[26] A. Semmeq, S. Ouaskit, A. Monari, M. Badawi, Ionization and fragmentation of uracil upon microhydration, Phys. Chem. Chem. Phys. 21 (2019) 4810–4821.
[27] S. Miertus, J. Tomasi, Approximate evaluations of the electrostatic free energy and internal changes in solution processes, Chem. Phys. 65 (1985) 239–245.
[28] M.J. Frisch, G.W. Trucks, H.B. Schlegel, G.E. Scuseria, M.A. Robb, J.R. Cheeseman, G. Scalmani, V. Barone, B. Mennucci, G.A. Petersson, H. Nakatsuji, M. Caricato, X. Li, H.P. Hratchian, A.F. Izmaylov, J. Bloino, G. Zheng, J.L. Sonnenberg, M. Hada, M. Ehara, K. Toyota, R. Fukuda, J. Hasegawa, M. Ishida, T. Nakajima, Y. Honda, O. Kitao, H. Nakai, T. Vreven, J.A. Montgomery Jr., J.E. Peralta, F. Ogliaro, M. Bearpark, J.J. Heyd, E. Brothers, K.N. Kudin, V.N. Staroverov, R. Kobayashi, J. Normand, K. Raghavachari, A. Rendell, J.C. Burant, S.S. Iyengar, J. Tomasi, M. Cossi, N. Rega, J.M. Millam, M. Klene, J.E. Knox, J.B. Cross, V. Bakken, C. Adamo, J. Jaramillo, R. Gomperts, R.E. Stratmann, O. Yazyev, A.J. Austin, R. Cammi, C. Pomelli, J.W. Ochterski, R.L. Martin, K. Morokuma, V.G. Zakrzewski, G.A. Voth, P. Salvador, J.J. Dannenberg, S. Dapprich, A.D. Daniels, O. Farkas, J.B. Foresman, J.V. Ortiz, J. Cioslowski, D.J. Fox, Gaussian 09, Revision A.1, Gaussian, Inc., Wallingford, 2009.
[29] V.K. Mavrodiev, M.F. Abdullin, D.V. Gamirova, E.M. Vyrypaev, I.I. Furlei, F.Z. Galin, Fragmentation process in phthalimide-and pyridine-2,3-dicarboimidoalkyl-α-diazoketones under resonant electron capture, Int. J. Mass Spectrom. 279 (2009) 37–40.
[30] C.B. Jacoby, M.L. Gross, R.L. Zey, The decomposition of N-(substituted benzalamino)phthalimide radical cations embody ion-neutral complexes and Stevenson's rule, J. Am. Soc. Mass Spectrom. 5 (1994) 837–844.
[31] J.L. Holmes, F. Benoit, The mass spectra of benzamide and thiobenzamide, Org. Mass Spectrom. 5 (1971) 525–530.